

Structure Prediction of Au₄₄(SR)₂₈: A Chiral Superatom Cluster

Yong Pei,* Sisi Lin, Jingcang Su, and Chunyan Liu

Department of Chemistry, Key Laboratory of Environmentally Friendly Chemistry and Applications of Ministry of Education, Xiangtan University, Hunan Province 411105, P. R. China

S Supporting Information

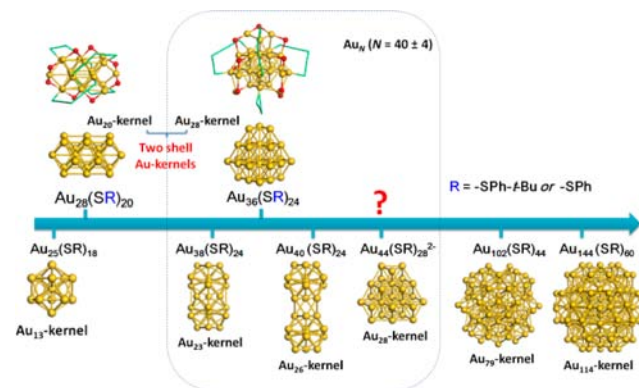
ABSTRACT: The structure of a thiolate-protected Au₄₄ cluster, [Au₄₄(SR)₂₈], is theoretically predicted via density functional theory calculations. Au₄₄(SR)₂₈ is predicted to contain a “two-shell” face-centered-cubic type of Au kernel and possess chirality. The predicted cluster structure is validated by comparison of optical absorption properties between theory and previous experiments, as well as energy evaluations. Based on the predicted cluster structure, the magic stability of Au₄₄(SR)₂₈ is understood from the superatom electronic configuration and formation of a unique double-helix superatom network inside.

Thiolate-protected gold nanoparticles (RS-AuNPs) or nanoclusters (NCs) are important types of self-assembled monolayer (SAM)-protected noble metal clusters. The synthesis and characterization of RS-AuNCs in the size range of 1–2 nm received intense research interest in the past decade.^{1–8} Determining the atomic structure of these NCs is a major challenge for both experiment and theory, which greatly hinders in-depth understanding of their structural evolution and size-dependent properties.

In recent years, significant progress was made in determining the total structure of RS-AuNPs from experiment and theory. In summary, after the breakthroughs of crystallization of Au₁₀₂(*p*-MBA)₄₄ (*p*MBA = *p*-mercaptobenzoic acid, SC₇O₂H₅)⁹ and Au₂₅(SCH₂CH₂Ph)₁₈[–],¹⁰ the structures of Au₃₈[–](SCH₂CH₂Ph)₂₄,¹¹ Au₂₈(SPh-*t*-Bu)₂₀,¹² and Au₃₆(SPh-*t*-Bu)₂₄¹³ were consecutively resolved via single-crystal X-ray diffraction. Based on the resolved structure of Au₁₀₂(*p*-MBA)₄₄ and Au₂₅(SCH₂CH₂Ph)₁₈[–], a heuristic structural rule that any thiolate-protected gold cluster can be viewed as the combination of an intact, highly symmetric Au core and a certain number of protecting staple motifs is summarized as well.^{14–19} In the past few years, this rule led to structural predictions of a variety of RS-AuNPs.^{15–19} Among these studies, the independent structural predictions of Au₃₈(SR)₂₄^{15a,16c} and Au₂₅(SR)₁₈^{–16b} from theory were very successful, which were both confirmed by experiments.^{10,11}

Here we report the structural prediction of Au₄₄(SR)₂₈, a magic-numbered gold cluster protected by all-aromatic thiophenolate ligands (-SPh).²⁰ The dianionic Au₄₄(SR)₂₈ has been widely cited as a superatom cluster with a unique 18e shell since its first synthesis in 2005,^{3,5,7,8,14–21} but determining an accurate atomic structure of Au₄₄(SR)₂₈ remains a grand challenge for both experiment and theory. Recently, the structural models were proposed for Au₄₄(SR)₂₈^{19f} and Au₄₀(SR)₂₄^{8b} based on the “general” trend that the inner Au kernels evolve from icosahedral atomic arrangement at smaller sizes to decahedral structures at

Scheme 1. Au Kernel Structures of Various Thiolate-Protected Gold Clusters That Have Been Either Resolved by Experiments or Predicted by Theory^a



^aIn the case of the “two-shell” Au kernels displayed above the arrow, thiolate groups in the second shell are removed for clarity.

larger ones.^{14–19} Nonetheless, one may find that some key parameters, such as the shape of the optical curve derived from the predicted cluster structures (for example, the recent prediction of Au₄₄(SR)₂₈^{19f}), do not agree satisfactorily with the experimental measurements. An interesting question is raised about whether the “general” structural trend derived from the Au₂₅, Au₃₈, and Au₁₀₂ clusters is adequate for understanding the structure of Au₄₄(SR)₂₈.

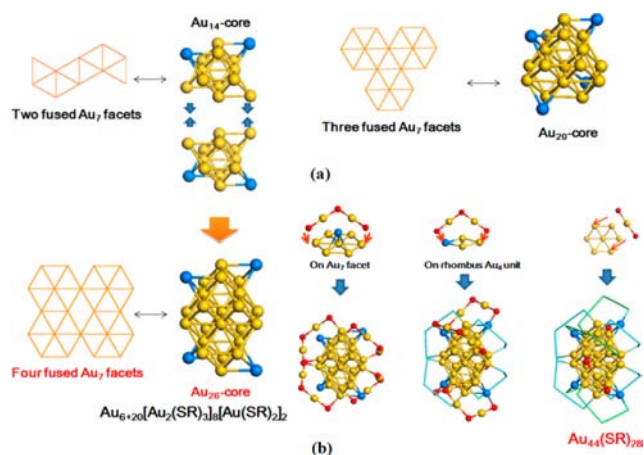
Recently, the structures of Au₂₈(SPh-*t*-Bu)₂₀¹² and Au₃₆(SPh-*t*-Bu)₂₄^{13a} clusters were successfully resolved. In Au₂₈ and Au₃₆ clusters, the unique “two-shell” face-centered-cubic (FCC)-type of Au kernels are observed for the first time, which are much different from the Au core structures in well-known Au₂₅, Au₃₈, and Au₁₀₂ clusters, as shown in Scheme 1.

The cluster composition of Au₄₄(SR)₂₈ is interesting in relation to Au₂₈(SPh-*t*-Bu)₂₀¹² and Au₃₆(SPh-*t*-Bu)₂₄.^{13a} First, the reported Au₄₄(SR)₂₈ cluster²⁰ has thiophenolate as protecting ligand, similar to the *p*-thiophenolate protecting ligand in Au₂₈ and Au₃₆ clusters. Second, the Au₄₄ cluster can evolve from the Au₂₈ cluster via sequential addition of [Au₈(SR)₄] units, i.e., Au₂₈(SR)₂₀ + [Au₈(SR)₄] → Au₃₆(SR)₂₄ + [Au₈(SR)₄] → Au₄₄(SR)₂₈. The close similarities in the compositions of Au₄₄, Au₃₆, and Au₂₈ clusters imply intrinsic connections of their structures, which inspire us to re-examine the structure of Au₄₄(SR)₂₈.

Received: September 21, 2013

Published: November 25, 2013

Scheme 2. (a) Au_{14} Core in $Au_{28}(SR)_{20}$ and Au_{20} Core in $Au_{36}(SR)_{24}$, and (b) Proposed Au_{26} Core and Assembly Process of $Au_{44}(SR)_{28}$ ^a



^aBlue balls denote the gold adatoms; red balls are S atoms.

Scheme 2a displays the divided inner Au core structures of $Au_{28}(SPh-t-Bu)_{20}$ and $Au_{36}(SPh-t-Bu)_{24}$ according to the “divide-and-protect” scheme.^{15,16} For example, $Au_{28}(SPh-t-Bu)_{20}$ and $Au_{36}(SPh-t-Bu)_{24}$ can be divided into $Au_{14}[Au_2(SR)_3]_4[Au_3(SR)_4]_2$ and $Au_{20}[Au_2(SR)_3]_8$, respectively. From Scheme 2a, the Au_{14} and Au_{20} cores both have hexagonal-like Au_7 facets covered by symmetrically distributed gold adatoms. On the basis of the configurations of Au_{14} and Au_{20} cores, we propose a Au_{26} core for $Au_{44}(SR)_{28}$. From Scheme 2b, the proposed Au_{26} core can be viewed as two Au_{14} cores fused by sharing a gold dimer, with four symmetrically distributed gold adatoms on four hexagonal Au_7 facets. The Au_{26} core is a reasonable candidate for building $Au_{44}(SR)_{28}$ according to the “divide-and-protect” scheme, e.g., $Au_{6+20}[Au_2(SR)_3]_8[Au(SR)_2]_2$ (displayed in Table S1). From the proposed Au_{26} core, we step-by-step wrap the dimeric and monomeric staple motifs through learning the structural features of $Au_{28}(SPh-t-Bu)_{20}$ and $Au_{36}(SPh-t-Bu)_{24}$ clusters (cf. Figure S1). From Scheme 2b, after adding eight

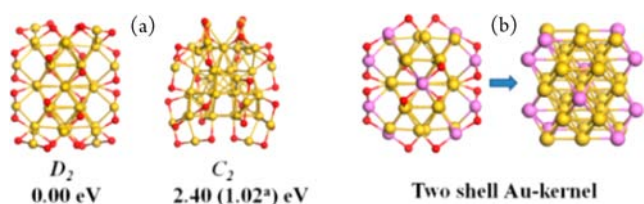


Figure 1. (a) Comparison of proposed structural models for the $Au_{44}(SR)_{28}$ cluster: left, present model; right, model from ref 19f. Red and yellow denote S and Au atoms, respectively; methyl groups are omitted for clarity. “In parentheses is given the relative energy of the dianionic cluster. (b) The “two-shell” Au kernel in $Au_{44}(SR)_{28}$. Pink balls denote second-shell Au atoms contributed from the staple motifs.

dimeric staple motifs upon four hexagonal Au_7 facets and four rhombus Au_4 units, two sets of unprotected gold atoms are left on both sides of the Au_{26} core. Two monomeric staple motifs are then added to passivate them.

Figure 1 shows the optimized cluster structure of $Au_{44}(SMe)_{28}$ ($-R$ is simplified as a methyl group). It contains a D_2 -symmetric Au-S framework and a “two-shell” Au kernel. The computational method and details are given in the Supporting Information.

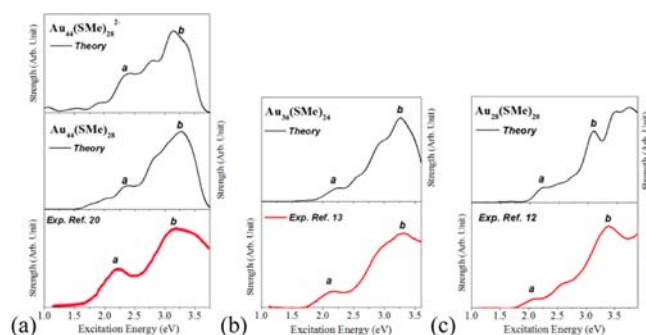
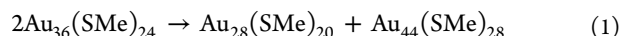


Figure 2. Comparison of theoretical optical absorption curves with the experimental ones for (a) $Au_{44}(SR)_{28}$ cluster in neutral and dianionic charge states, (b) $Au_{36}(SR)_{24}$ cluster, and (c) $Au_{28}(SR)_{20}$ cluster.

Energy computations at the PBE/TZP level indicate that the currently predicted structure is more stable by 2.4 or 1.02 eV in neutral and dianionic states, respectively, than the structure recently predicted by Jiang et al.^{19f} Note that Jiang’s Au_{44} model is based on the structural rule derived from Au_{25} , Au_{38} , and Au_{102} clusters, which contains an intact Au_{28} core.^{19f}

The optical absorption properties of optimized $Au_{44}(SMe)_{28}$ are further examined. In Figure 2a, simulated optical absorption curves are displayed for $Au_{44}(SMe)_{28}$ in both neutral and dianionic states. The simulated optical absorption curve of neutral $Au_{44}(SMe)_{28}$ is found to be in good agreement with previous experimental results.²⁰ The experimental optical gap (~ 1.5 eV) as well as two feature absorption peaks (*a* and *b*) at nearly 2.2 and 3.2 eV are well reproduced. Nonetheless, the dianionic cluster, i.e., $Au_{44}(SMe)_{28}^{2-}$, has a much smaller HOMO/LUMO gap of ~ 0.3 eV. Weak absorption peaks are found in the lower excitation energy region (< 1.5 eV). Figure 2b,c also displays the simulated optical absorption curves of $Au_{28}(SMe)_{20}$ and $Au_{36}(SMe)_{24}$ clusters. The good agreement between theoretical and experimental optical absorption curves of Au_{28} and Au_{36} clusters indicates the current theoretical methods can well reproduce optical properties of thiolated gold clusters.

Besides examining optical absorption properties, we evaluate the relative stability of the predicted structure of $Au_{44}(SR)_{28}$ against $Au_{36}(SR)_{24}$ and $Au_{28}(SR)_{20}$ as well. Equation 1 shows



how two $Au_{36}(SR)_{24}$ clusters can convert into a $Au_{28}(SR)_{20}$ and a $Au_{44}(SR)_{28}$. Note the three clusters in eq 1 are all of neutral charge states: if $Au_{44}(SR)_{28}$ is negatively charged, the charge-balance will break. Energy computations (PBE/TZP level) indicate that the conversion of two $Au_{36}(SMe)_{24}$ clusters into a $Au_{44}(SMe)_{28}$ and a $Au_{28}(SMe)_{20}$ is slightly endothermic by 0.58 eV, suggesting the Au_{44} cluster has relatively high thermodynamic stabilities against Au_{36} and Au_{28} clusters.

The present theoretical results raise a question about the charge state of $Au_{44}(SR)_{28}$, which was previously suggested to be a dianionic cluster.²⁰ An 18e shell has been widely used to explain the magic stability of $Au_{44}(SR)_{28}^{2-}$.^{3,5,7,8,14–21} At present, our theoretical results indicate the dianionic $Au_{44}(SR)_{28}$ has a quite small HOMO/LUMO gap (~ 0.3 eV). The properties of neutral $Au_{44}(SR)_{28}$ show much better agreement with previous experimental results than the dianionic one, such as the optical gap and shape of optical curve displayed in Figure 2a, and the revealed evolution trend and possible interconversion of Au_{28} ,

Au₃₆ and Au₄₄ clusters from eq 1 support neutral Au₄₄(SR)₂₈. We hope future experiments can verify the charge state of Au₄₄(SR)₂₈. We note a new synthesis of neutral Au₄₄(SR)₂₈ (R = SPh-*t*-Bu) was achieved recently, which confirms our theoretical prediction of the charge state of Au₄₄(SR)₂₈.²²

Prediction of the cluster structure of Au₄₄(SR)₂₈ allows us to further explore the intrinsic connections of properties between the Au₄₄ cluster and the recently discovered Au₂₈ and Au₃₆ clusters. A striking structural feature of Au₂₈(SR)₂₀ and Au₃₆(SR)₂₄ is the formation of unique FCC-type “two-shell” Au kernels, i.e., Au₂₀ kernel and Au₂₈ kernel,^{12,13} respectively. From Figures 1 and 3, the Au₄₄(SR)₂₈ contains a “two-shell” Au₃₆ kernel as well, which demonstrates a clear trend in evolution from Au₂₈ and Au₂₀ kernels. First, the Au₃₆ kernel can be viewed as either the fusion of two Au₂₀ kernels sharing square (100) facets or the sequentially addition of a boat-like Au₈ cap at the bottom and top of a Au₂₀ kernel. Second, the Au₃₆ kernel has an edge-shared bi-tetrahedron Au₆ core, with an evolution pattern of Au dimer (in Au₂₀ kernel) → Au tetrahedron (in Au₂₈ kernel) → edge-shared Au bi-tetrahedron (in Au₃₆ kernel). Third, the second shell of Au₃₆ kernel has similar triangular (111) and square (100) facets to those of Au₂₀ and Au₂₈ kernels. The unique structure and evolution patterns of the three Au kernels suggest Au₂₈(SR)₂₀, Au₃₆(SR)₂₄, and Au₄₄(SR)₂₈ constitute a new family of thiolate-protected gold clusters. During the submission of our manuscript, Zeng et al. made a similar prediction of FCC-type Au kernel in Au₄₄(SR)₂₈ but did not address the structure of the Au₄₄ cluster, nor its relative stability and structure-dependent properties such as chirality and superatom properties.²²

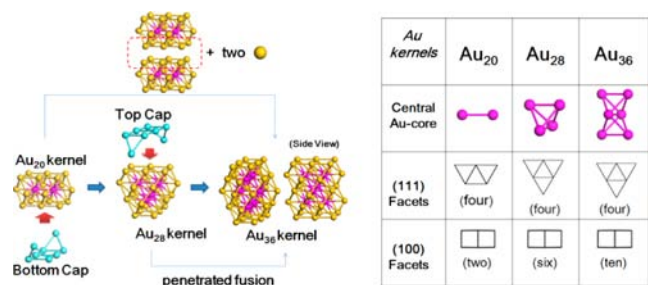


Figure 3. Left: Evolution of three “two-shell” Au kernels in Au₂₈(SR)₂₀, Au₃₆(SR)₂₄, and Au₄₄(SR)₂₈ clusters, respectively. Right: Comparison of structural features of three Au kernels.

The magic stability of Au₄₄(SR)₂₈ is further addressed in terms of both superatom complex (SAC)³ and superatom network (SAN)²³ models through analyzing the electronic structure of Au core. From Figure 1, Au₄₄(SR)₂₈ is predicted to contain a Au₂₆ core (protected by 10 staple motifs), which can be considered as Au₂₆¹⁰⁺ according to the SAC model. The electronic structure analysis shows the Au₂₆¹⁰⁺ possesses delocalized 1S, 1P, and 1D superatom orbitals. As shown in Figure 4a, the 1P and 1D orbitals in Au₂₆¹⁰⁺ are both non-degenerate, due to the nonspherical shape of the Au core. The HOMO Kohn–Sham (KS) orbital is the highest occupied 1D orbital, and the LUMO KS orbital corresponds to the unoccupied 1D orbital. The Au₂₆¹⁰⁺ thus has a 1S²1P⁶1D⁸ electronic configuration. The electronic structures of Au₁₄⁶⁺ and Au₂₀⁸⁺ in Au₂₈(SR)₂₀ and Au₃₆(SR)₂₄ clusters are also examined for comparison (Figure S2). The Au₁₄⁶⁺ and Au₂₀⁸⁺ demonstrate delocalized superatom orbitals as well, in partial agreement with the recent theoretical analysis.^{13a,21a} In particular, the Au₂₀⁸⁺ core in the Au₃₆ cluster has a more clearly

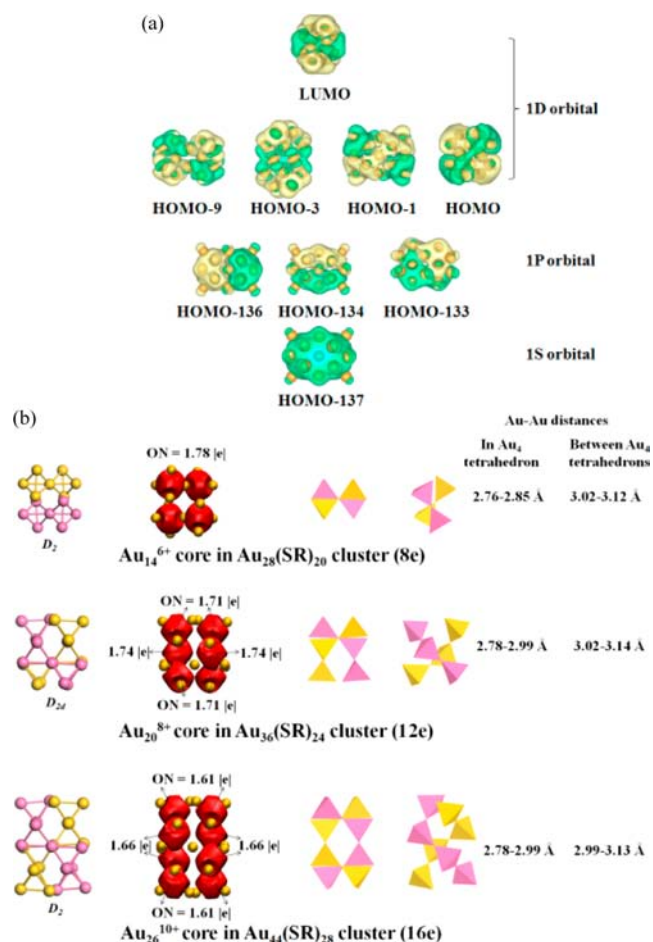


Figure 4. (a) Superatomic orbitals in Au₂₆¹⁰⁺. (b) AdNDP analysis of Au²⁺ cores in Au₄₄(SR)₂₈, Au₃₆(SR)₂₄, and Au₂₈(SR)₂₀. ON denotes the occupation number of the 4c-2e bond. Polyhedron denotes the superatom Au₄ unit.

defined shape of superatom orbitals than the other two Au cores due to the nearly spherical distribution of gold atoms.

On the other hand, geometric analysis of the Au₂₆ core indicates it contains a network of eight Au₄ tetrahedrons. From Figure 4b, the Au–Au bond lengths within the Au₄ tetrahedrons are in the range of 2.78–2.99 Å. The Au–Au distances between two nearby tetrahedrons within different tetrahedron chains are in the range of 2.99–3.13 Å. In view of these geometric features, we suspect the Au₂₆ core can also be considered as a network of eight 4c-2e tetrahedron Au₄ superatoms according to the SAN model proposed recently.²³ To confirm the speculation, we performed chemical bond analysis of Au₂₆¹⁰⁺ using the adaptive natural density partitioning (AdNDP) method.²⁴ AdNDP analysis is an efficient tool to explore the multicentered bonds of atomic clusters via a scheme of orbital transformations. From Figure 4b, eight 4c-2e bonds are found within Au₂₆¹⁰⁺, which are divided into two groups with slightly different occupancy numbers (ON = 1.66 and ON = 1.61, respectively). The Au₂₆¹⁰⁺ can be viewed as a network of eight tetrahedron Au₄ superatoms according to the SAN model.^{23a}

A striking feature of the superatom network in Au₂₆¹⁰⁺ is that eight tetrahedron Au₄ units arrange into a double-helix configuration. The tetrahedron Au₄ superatoms in each chain are conjugated via a Au vertex. This kind of superatom network is different from those discovered in Au₂₀(SR)₁₆ and Au₂₄(SR)₂₀; the latter ones have a nonconjugate arrangement of two

tetrahedron Au₄ superatoms.²³ From Figure 4b, we find that the Au cores in Au₂₈(SR)₂₀ and Au₃₆(SR)₂₄ clusters also contain two strings of conjugated tetrahedron Au₄ superatoms. An evolution trend of superatom networks in the three Au cores is clearly found (Figure 4b), which again shows close relations of Au₂₈, Au₃₆, and Au₄₄ clusters. Here we note the SAN explanation is not in conflict with the SAC model. The SAN model focuses on the delocalized multicentered bonding within a cluster. For example, ten 4c-2e bonds are found within the magic stable tetrahedron Au₂₀ cluster.^{24b} The existence of 13c-2e superatom bonds in the bi-icosahedron Au₂₃ core of Au₃₈(SR)₂₄ was also revealed recently.^{23b} Those studies both provided new insights into the magic stability of gold clusters with or without ligand protections.^{24c}

Finally, the D₂-symmetric structure of Au₄₄(SR)₂₈ prompted us to examine its chiral properties, which were not discussed previously by either theory or experiment. The simulated circular dichroism (CD) spectra indicate the Au₄₄(SR)₂₈ is a chiral cluster, which exhibits strong chiral responses in range of excitation energy of 1.5–3.5 eV (cf. Figure S3). The strongest rotatory strength of Au₄₄(SMe)₂₈ is ~4 times higher than that of Au₂₈(SMe)₂₀¹² and also much higher than that of Au₃₈(SMe)₂₄.^{16c} The observed strong chiral response of Au₄₄(SMe)₂₈ can be used as an alternative indicator to verify the predicted structure. We propose the separation of enantiomers and the use of chiral ligand will be promising ways to detect the chiral properties of Au₄₄ clusters.

In summary, the structure of a Au₄₄(SR)₂₈ cluster is predicted. The magic stability of Au₄₄(SR)₂₈ is understood from the superatom electronic configuration and tetrahedral Au₄ superatom network of the Au core. On basis of the predicted structure, a unified view of structural evolution and superatomic properties of Au₄₄(SR)₂₈ and the recently discovered Au₃₆(SR)₂₄ and Au₂₈(SR)₂₀ clusters is provided, which proposes three clusters constitute a new family of thiolate-protected gold clusters.

■ ASSOCIATED CONTENT

Supporting Information

Computational details and characterization data. This material is available free of charge via the Internet at <http://pubs.acs.org>.

■ AUTHOR INFORMATION

Corresponding Author

yypnku78@gmail.com

Notes

The authors declare no competing financial interest.

■ ACKNOWLEDGMENTS

This work is supported by NSFC (21103144, 21373176), Hunan Provincial Natural Science Foundation of China (12JJ7002, 12JJ1003), and Scientific Research Fund of Hunan Provincial Education Department (13A100).

■ REFERENCES

- (1) (a) Brust, M.; Walker, M.; Bethell, D.; Schiffrin, D. J.; Whyman, R. *J. Chem. Soc., Chem. Commun.* **1994**, 801. (b) Whetten, R. L.; Khoury, J. T.; Alvarez, M. M.; Murthy, S.; Vezmar, I.; Wang, Z. L.; Stephens, P. W.; Cleveland, C. L.; Luedtke, W. D.; Landman, U. *Adv. Mater.* **1996**, *8*, 428.
- (2) Parker, J. F.; Fields-Zinna, C. A.; Murray, R. W. *Acc. Chem. Res.* **2010**, *43*, 1289.
- (3) (a) Häkkinen, H. *Nature Chem.* **2012**, *4*, 443. (b) Walter, M.; Akola, J.; Lopez-Acevedo, O.; Jadzinsky, P. D.; Calero, G.; Ackerson, C. J.;

Whetten, R. L.; Grönbeck, H.; Häkkinen, H. *Proc. Natl. Acad. Sci. U.S.A.* **2008**, *105*, 9157. (c) Häkkinen, H. *Chem. Soc. Rev.* **2008**, *37*, 1847.

- (4) Jin, R. *Nanoscale* **2010**, *2*, 343.
- (5) (a) Tsunoyama, H.; Nickut, P.; Negishi, Y.; Al-Shamery, K.; Matsumoto, Y.; Tsukuda, T. *J. Phys. Chem. C* **2007**, *111*, 4153. (b) Maity, P.; Xie, S.; Yamauchi, M.; Tsukuda, T. *Nanoscale* **2012**, *4*, 4027.
- (6) Qian, H.; Zhu, M.; Wu, Z.; Jin, R. *Acc. Chem. Res.* **2012**, *45*, 1470 and references therein.
- (7) (a) Dass, A. *J. Am. Chem. Soc.* **2009**, *131*, 11666. (b) Nimmala, P. R.; Dass, A. *J. Am. Chem. Soc.* **2011**, *133*, 9175.
- (8) (a) Knoppe, S.; Dolamic, I.; Dass, A.; Burgi, T. *Angew. Chem., Int. Ed.* **2012**, *51*, 7589. (b) Malola, S.; Lehtovaara, L.; Knoppe, S.; Hu, K.-J.; Palmer, R. E.; Bürgi, T.; Häkkinen, H. *J. Am. Chem. Soc.* **2012**, *134*, 19560.
- (9) Jadzinsky, P. D.; Calero, G.; Ackerson, C. J.; Bushnell, D. A.; Kornberg, R. D. *Science* **2007**, *318*, 430.
- (10) (a) Heaven, M. W.; Dass, A.; White, P. S.; Holt, K. M.; Murray, R. W. *J. Am. Chem. Soc.* **2008**, *130*, 3754. (b) Zhu, M.; Aikens, C. M.; Hollander, F. J.; Schatz, G. C.; Jin, R. *J. Am. Chem. Soc.* **2008**, *130*, 5883.
- (11) Qian, H.; Eckenhoff, W. T.; Zhu, Y.; Pintauer, T.; Jin, R. *J. Am. Chem. Soc.* **2010**, *132*, 8280.
- (12) Zeng, C.; Li, T.; Das, A.; Rosi, N. L.; Jin, R. *J. Am. Chem. Soc.* **2013**, *135*, 10011.
- (13) (a) Zeng, C.; Qian, H.; Li, T.; Li, G.; Rosi, N.; Yoon, B.; Whetten, R.; Landman, U.; Jin, R. *Angew. Chem., Int. Ed.* **2012**, *51*, 13114. (b) Zeng, C.; Liu, C.; Pei, Y.; Jin, R. *ACS Nano* **2013**, *7*, 6138.
- (14) (a) Pei, Y.; Zeng, X. C. *Nanoscale* **2012**, *4*, 4054. (b) Jiang, D. *Nanoscale* **2013**, *5*, 7149.
- (15) (a) Pei, Y.; Gao, Y.; Zeng, X. C. *J. Am. Chem. Soc.* **2008**, *130*, 7830. (b) Pei, Y.; Gao, Y.; Zeng, X. C. *J. Am. Chem. Soc.* **2009**, *131*, 13619. (c) Pei, Y.; Pal, R.; Liu, C.; Gao, Y.; Zhang, Z.; Zeng, X. C. *J. Am. Chem. Soc.* **2012**, *134*, 3015.
- (16) (a) Häkkinen, H.; Walter, M.; Grönbeck, H. *J. Phys. Chem. B* **2006**, *110*, 9927. (b) Akola, J.; Walter, M.; Whetten, R. L.; Häkkinen, H.; Grönbeck, H. *J. Am. Chem. Soc.* **2008**, *130*, 3756. (c) Lopez-Acevedo, O.; Tsunoyama, H.; Tsukuda, T.; Häkkinen, H.; Aikens, C. M. *J. Am. Chem. Soc.* **2010**, *132*, 8210. (d) Lopez-Acevedo, O.; Akola, J.; Whetten, R. L.; Grönbeck, H.; Häkkinen, H. *J. Phys. Chem. C* **2009**, *113*, 5035.
- (17) (a) Aikens, C. M. *J. Phys. Chem. Lett.* **2011**, *2*, 99. (b) Provorse, M. R.; Aikens, C. M. *J. Am. Chem. Soc.* **2010**, *132*, 1302. (c) Aikens, C. M. *J. Phys. Chem. A* **2009**, *113*, 10811.
- (18) (a) Sánchez-Castillo, A.; Noguez, C.; Garzón, I. L. *J. Am. Chem. Soc.* **2010**, *132*, 1504. (b) Tlahuice, A.; Garzón, I. L. *Phys. Chem. Chem. Phys.* **2012**, *14*, 3737.
- (19) (a) Jiang, D.; Whetten, R. L.; Luo, W.; Dai, S. *J. Phys. Chem. C* **2009**, *113*, 17291. (b) Jiang, D.; Overbury, S. H.; Dai, S. *J. Am. Chem. Soc.* **2013**, *135*, 8786. (c) Jiang, D. *Chem.—Eur. J.* **2011**, *17*, 12289. (d) Jiang, D.; Chen, W.; Whetten, R. L.; Chen, Z. *J. Phys. Chem. C* **2009**, *113*, 16983. (e) Jiang, D.; Tiago, M. L.; Luo, W.; Dai, S. *J. Am. Chem. Soc.* **2008**, *130*, 2777. (f) Jiang, D.; Walter, M.; Akola, J. *J. Phys. Chem. C* **2010**, *114*, 15883.
- (20) Price, R. C.; Whetten, R. L. *J. Am. Chem. Soc.* **2005**, *127*, 13750.
- (21) (a) Knoppe, S.; Malola, S.; Lehtovaara, L.; Burgi, T.; Häkkinen, H. *J. Phys. Chem. A* **2013**, *117*, 10526. (b) Yang, H.; Wang, Y.; Huang, H.; Gell, L.; Lehtovaara, L.; Malola, S.; Häkkinen, H.; Zheng, N. *Nature Commun.* **2013**, *4*, 2422.
- (22) Zeng, C.; Chen, Y.; Li, G.; Jin, R. *Chem. Commun.* **2014**, *50*, 55.
- (23) (a) Cheng, L.; Yuan, Y.; Zhang, X.; Yang, J. *Angew. Chem., Int. Ed.* **2013**, *52*, 9035. (b) Cheng, L.; Ren, C.; Zhang, X.; Yang, J. *Nanoscale* **2013**, *5*, 1475.
- (24) (a) Zubarev, Yu. D.; Boldyrev, A. I. *Phys. Chem. Chem. Phys.* **2008**, *10*, 5207. (b) Lu, T.; Chen, F. *J. Comput. Chem.* **2012**, *33*, 580. (c) Zubarev, D. Y.; Boldyrev, A. I. *J. Phys. Chem. A* **2009**, *113*, 866.